

A UNIVERSAL VELOCITY DISPERSION PROFILE FOR PRESSURE SUPPORTED SYSTEMS: EVIDENCE FOR MONDIAN GRAVITY ACROSS 7 ORDERS OF MAGNITUDE IN MASS

R. DURAZO¹, X. HERNANDEZ¹, B. CERVANTES SODI² AND S. F. SÁNCHEZ¹

¹Instituto de Astronomía, Universidad Nacional Autónoma de México, Apartado Postal 70–264 C.P. 04510 México D.F. México.

²Instituto de Radioastronomía y Astrofísica, Universidad Nacional Autónoma de México, Campus Morelia, 58090 Morelia, Michoacán, México.

Abstract

For any MONDian extended theory of gravity where the rotation curves of spiral galaxies are explained through a change in physics rather than the hypothesis of dark matter, a generic dynamical behavior is expected for pressure supported systems: an outer flattening of the velocity dispersion profile occurring at a characteristic radius, where both the amplitude of this flat velocity dispersion and the radius at which it appears are predicted to show distinct scalings with the total mass of the system. By carefully analyzing the dynamics of globular clusters and elliptical galaxies, we are able to significantly extend the astronomical diversity of objects in which MONDian gravity has been tested, from spiral galaxies, to the much larger mass range covered by pressure supported systems. We show that a universal projected velocity dispersion profile accurately describes various classes of pressure supported systems, and further, that the expectations of extended gravity are met, across seven orders of magnitude in mass. These observed scalings are not expected under dark matter cosmology, and would require particular explanations tuned at the scales of each distinct astrophysical system.

Keywords: gravitation — stars:kinematics and dynamics — galaxies:star clusters:general — galaxies: fundamental parameters — galaxies: kinematics and dynamics

1. INTRODUCTION

Within the context of modified gravity theories constructed to yield galactic dynamics in the absence of dark matter, one of the most convincing supporting arguments comes from the success of MOND in reproducing rotation curves of spiral galaxies (Milgrom 1983; Swaters et al. 2010; McGaugh 2012). Both the flatness of the observed spiral rotation curves and the scaling of the asymptotic rotation with the fourth root of the total baryonic content, i. e. the Tully-Fisher relation, can be accurately reproduced across spiral galaxy sizes and types, as well as the overall shapes and correlations between observed features in the baryonic distribution and small kinematic irregularities (Sanders & McGaugh 2002; Famaey & McGaugh 2012; Rodrigues 2014; Lelli et al. 2016). However, such successful tests are restricted to the range of mass scales and morphology of spiral galaxies.

To test the validity (or lack thereof) of MONDian gravity schemes, it is desirable to extend the diversity of astrophysical systems over which these ideas can be probed. To do this, we give the expected kinematic profiles for two different types of pressure supported systems, astrophysical objects with baryonic masses span-

ning from $10^4 M_\odot$ for globular clusters, to $10^{11} M_\odot$ for elliptical galaxies.

By the term MONDian gravity we shall refer to any extended gravity theory where at $a > a_0$ scales Newtonian gravity is recovered, while the $a < a_0$ regime reproduces MOND dynamics, at the $v \ll c$ limit, where a_0 is Milgrom’s acceleration of $1.2 \times 10^{-10} m/s^2$ (Bekenstein 2004; Capozziello & De Laurentis 2011; Mendoza et al. 2013; Verlinde 2016). Generically for such theories, beyond a radius given by $R_M = (GM/a_0)^{1/2}$, centrifugal equilibrium velocities will become flat at a level of $V = (GMa_0)^{1/4}$ (Milgrom 1983). Similarly, for pressure supported systems, beyond around R_M , velocity dispersion profiles will stop falling along Newtonian expectations and flatten out at a level of $\sigma_\infty = V/3^{1/2}$, with M the total baryonic mass of a rapidly converging astrophysical system (Milgrom 1984; Hernandez & Jimenez 2012).

Recently, McGaugh et al. (2016) and Lelli et al. (2016) used the SPARC rotation curve and photometry database, to show that the baryonic mass distribution alone directly determines the resulting acceleration, along Newtonian expectations in the high acceleration regime, and along MONDian ones when $a < a_0$. A

similar study reaching conclusions also in support of MONDian dynamics, but using structural, dynamical and mass determinations for a range of elliptical galaxies is that of Dabringhausen et al. (2016). Baryonic mass determination in the above studies however, are subject to numerous assumptions, as well as uncertainties and systematics, which vary for differing classes of astrophysical systems. Hard to determine gas fractions, star formation histories, the presence of multiple and complex stellar populations and unknown stellar mass functions imply mass to light ratios and their radial variations are subject to large empirical errors.

Here we take a complementary approach, using only kinematical data and avoiding any dynamical physical assumptions or mass estimates in deriving the parameters we study, concentrating merely on the shape of observed projected velocity dispersion profiles. The expected theoretical scalings of both R_M and σ_∞ with M imply the mass can be eliminated to obtain $R_M \propto \sigma_\infty^2$, a relation between the parameters of the directly observable velocity dispersion profiles which can now be directly tested.

By analysing velocity dispersion profiles from Galactic globular clusters recently observed by Scarpa et al. (2007a; 2007b), Scarpa & Falomo (2010) and Scarpa et al. (2011), henceforth the Scarpa et al. group, and Lane et al. (2009), Lane et al. (2010a; 2007b) and Lane et al. (2011), henceforth the Lane et al. group, and elliptical galaxies having high quality 2D kinematics by Sánchez et al. (2016b), using data from the CALIFA project, (Sánchez et al. 2012; Walcher et al. 2014; Sánchez et al. 2016a), we show that a universal projected velocity dispersion profile $\sigma(R) = \sigma_0 e^{-(R/R_\sigma)^2} + \sigma_\infty$ adequately serves to model the two distinct classes of astrophysical systems. Further, a scaling of $R_M \propto \sigma_\infty^n$ ensues, with $n = 1.89 \pm 0.32$, compatible with the generic expectations of MONDian gravity models of $n = 2$.

In section (2) we present the development of simple first order predictions for the large scale velocity dispersion expected under MONDian gravity, and the corresponding scalings between the parameters describing such velocity dispersion profiles for pressure supported systems. Section (3) includes a description of the data used for sets of velocity dispersion profiles for globular clusters and elliptical galaxies, together with the fitting procedure and parameters obtained for the universal velocity dispersion profile proposed. In section (4) we show how the two sets of systems treated, spanning seven orders of magnitude in mass, follow the proposed universal velocity dispersion profile, and show also how the flattening radii follow an overall scaling consistent with being proportional to the square of the asymptotic velocity dispersion, as predicted generically under MONDian gravity. Section (5) summarizes our conclusions.

2. MONDIAN THEORETICAL EXPECTATIONS

Thinking of modified gravity in terms of a Newtonian force law implies a change of regime from the Newtonian expression of $F_N = GM/r^2$ to $F_M = (GMa_0)^{1/2}/r$, occurring at scales of $R_M = (GM/a_0)^{1/2}$, if one wants to model observed galactic dynamics in the absence of any dark matter (Milgrom 1983). The details of the transition are not clear, beyond the requirements from consistency with solar system dynamics (Mendoza et al. 2011), Milky Way rotation curve comparisons (Famaey & Binney 2005) and Galactic globular cluster modelling (Hernandez et al. 2012), for the transition to be fairly abrupt. Under such schemes, centrifugal equilibrium velocities will tend to the Tully-Fisher value of:

$$V = (GMa_0)^{1/4}, \quad (1)$$

for test particles orbiting a total baryonic mass M . Under the MONDian regime, the relation between centrifugal equilibrium velocities and isotropic velocity dispersion will be only slightly modified with respect to the Newtonian case, to yield:

$$\sigma_\infty = V/\sqrt{3}, \quad (2)$$

e.g. Milgrom (1984), Hernandez & Jimenez (2012). Thus, we can write the isotropic Maxwellian velocity dispersion of a pressure supported system in the MONDian regime as:

$$\sigma_\infty^2 = \frac{1}{3}(GMa_0)^{1/2}. \quad (3)$$

In order to extend the range over which MONDian dynamics can be tested to the much larger ones over which pressure supported systems appear, would require observations of σ_∞ and independent inferences of the total baryonic mass of various systems, to directly test the validity of Equation (3). Any such undertaking will be hindered by the large theoretical uncertainties in total (and radially changing) mass to light ratios, uncertain gas fractions, and details of the relevant IMFs and star formation histories, which to make matters worse, vary significantly from the “simple” cases of globular clusters to the more complex histories of elliptical galaxies. One can circumvent such uncertainties and obtain a simpler empirical test by eliminating M from the above equation in favor of R_M to yield:

$$R_M = \frac{3\sigma_\infty^2}{a_0}, \quad (4)$$

which in astrophysical units reads:

$$\left(\frac{R_M}{pc}\right) = 0.81 \left(\frac{\sigma_\infty}{km/s}\right)^2. \quad (5)$$

The above expression now relates only features of the kinematic velocity dispersion profile of an astronomical system, as σ_∞ will be the large scale asymptotic projected velocity dispersion profile, and R_M will be the radial scale at which the velocity dispersion profile becomes flat. The above will only make any sense if observed velocity dispersion profiles do indeed show such morphology, for a decline in an inner Newtonian region, and a transition to a flat velocity dispersion regime on crossing the R_M threshold.

We are inspired to attempt such a comparison across the range of scales covered by pressure supported systems by recent results coming from the observed velocity dispersion profiles of Galactic globular clusters (Scarpa et al. 2010; Scarpa & Falomo 2011) showing precisely such a morphology, and recently shown to comply with Tully-Fisher MONDian expectations (Hernandez et al. 2013a). Further, Desmond (2017) recently demonstrated through an extensive sample of rotation curve observations and baryonic mass inferences across sizes and galactic types, that the inferred mass discrepancy acceleration relation is consistent with MONDian expectations.

In the following section we show a number of velocity dispersion profiles having precisely the morphology described above, for Galactic globular clusters and elliptical galaxies, which in Section 4 we compare to the expectations of Equation 5.

Notice also that multiplying Equations (3) and (4), and substituting M on the right hand side for σ_∞ , the resulting combination of parameters $R_M\sigma_\infty^2 = GM/3$ is highly reminiscent of the corresponding Newtonian expression, changing R_M for the half mass radius, and σ_∞ for the central velocity dispersion of a purely Newtonian system (Cappellari et al. 2006; Wolf et al. 2010).

In the above we have assumed that the total baryonic mass has essentially converged, and on reaching the flat dispersion velocity region the potential of the system in question can be treated as a point mass, in consistency with the validity of Newton's theorems for spherically symmetric mass distributions also under MONDian gravity (e.g. Mendoza et al. 2011), and that the dynamical tracers from which σ_∞ is calculated behave as test particles. Although this will never be strictly true, it will hold to a good approximation, given the very centrally concentrated mass profiles of e.g. Galactic globular clusters and the inferred density profiles of close to the de Vaucouleurs surface brightness of elliptical galaxies. Indeed, pressure supported systems have been accurately modeled recently in the MONDian regime reproducing simultaneously the observed surface brightness profiles and the measured velocity dispersion ones, e.g. Galactic globular clusters by Gentile et al. (2010), the giant elliptical galaxy NGC4649 by Jimenez et al. (2013)

and tenuous galactic stellar halos by Hernandez et al. (2013b), all in absence of any otherwise dominant dark matter component. More recently, Chae & Gong (2015) studied the predicted distribution of velocity dispersion profiles (VDP) for elliptical galaxies and found that their MONDian models could reproduce the observed distribution of VDP slopes requiring only the observed stellar mass, without any dark matter, and Tian & Ko (2016) concluded that the dynamics of seven elliptical galaxies, as traced by stellar and planetary nebulae, could be well explained by MOND. The issue remains controversial, as some studies have found dark matter halos to be a better fit than MOND in elliptical galaxies (Richtler et al. 2008; Samurović 2014, 2016).

3. EMPIRICAL VELOCITY DISPERSION PROFILES

3.1. Galactic globular clusters

In data recently available from the Scarpa et al. group and the Lane et al. group, not only the central values, but the radial projected velocity dispersion profiles for several systems have been published, extending out to several half-light radii. As first mentioned by the Scarpa et al. group, a flattening of the velocity dispersion profiles for Galactic globular clusters appears on crossing the a_0 acceleration threshold, in accordance with MONDian gravity expectations. In Hernandez & Jimenez (2012) some of us recently modeled the above globular cluster data to construct self-gravitating models for the systems studied, where both the projected surface brightness profiles and the observed velocity dispersion profiles have been accurately reproduced, using a modified gravity force law of the type described in section (2). Further, in Hernandez et al. (2013a) we showed that the asymptotic velocity dispersion values for the clusters treated actually match the expected scaling of $\sigma_\infty \approx (GMa_0)^{1/4}$ of MONDian gravity, through comparing with stellar synthesis models tuned to the ages and metallicities of each of the individual globular clusters studied. In the above works we also showed that an empirical projected velocity dispersion profile of the form:

$$\sigma(R) = \sigma_0 e^{-(R/R_\sigma)^2} + \sigma_\infty \quad (6)$$

serves to accurately model the reported velocity dispersion profiles of Galactic globular clusters. In Equation (6) σ_∞ is the asymptotic value for the system's velocity dispersion, the central value for this quantity is given by $\sigma(0) = \sigma_0 + \sigma_\infty$, and R_σ gives a transition radius beyond which the asymptote is rapidly approached.

Here we include again the fits to the data of the Scarpa et al. and Lane et al. groups to Equation (6). We use a non-linear least squares Levenberg-Marquardt al-

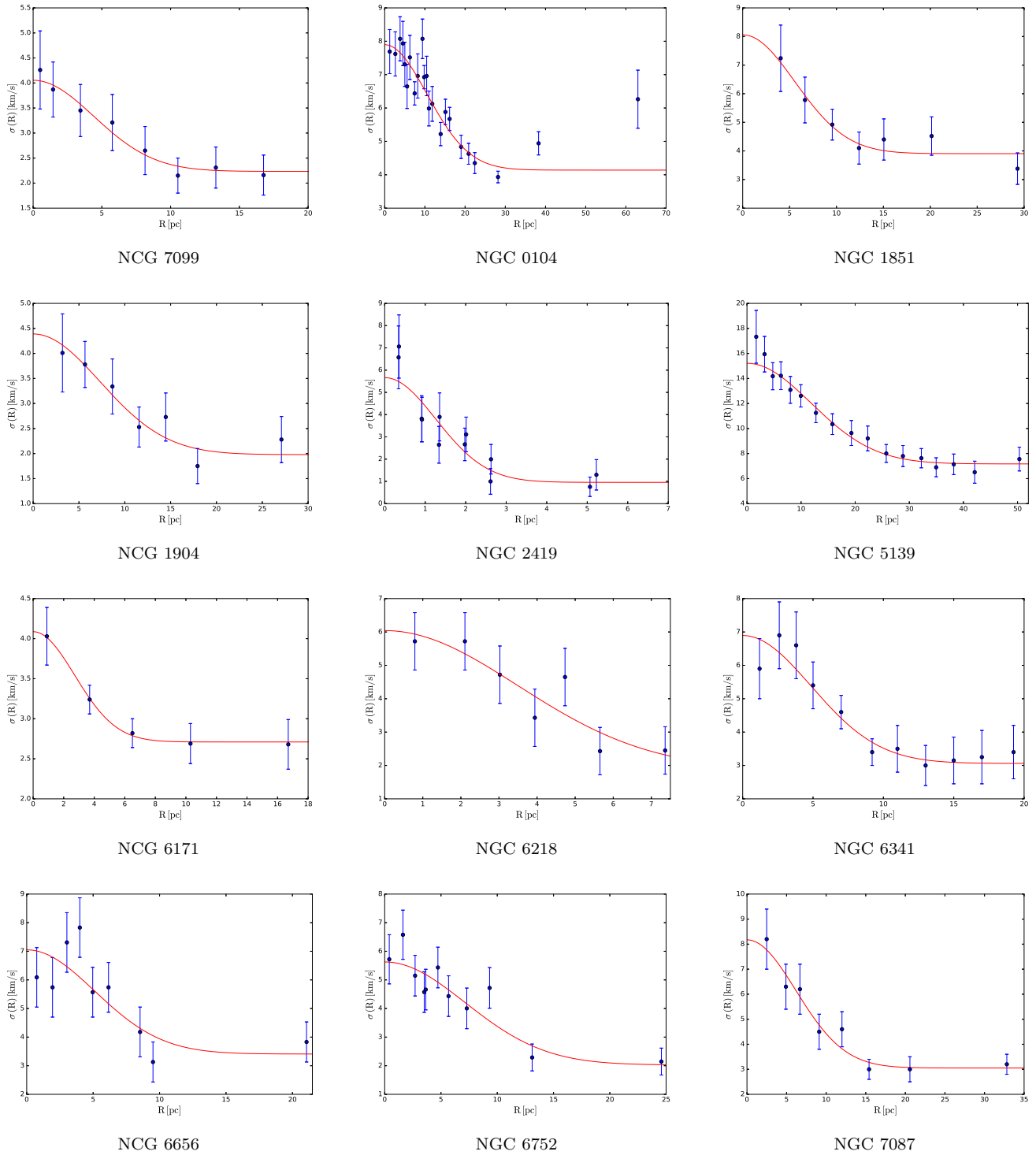


Figure 1. Projected velocity dispersion profiles for the 12 Galactic globular clusters of our sample, as a function of radial distance in the system, with vertical error bars showing the 1σ dispersion at each radial bin. The solid curve gives the best fit to the universal profile proposed.

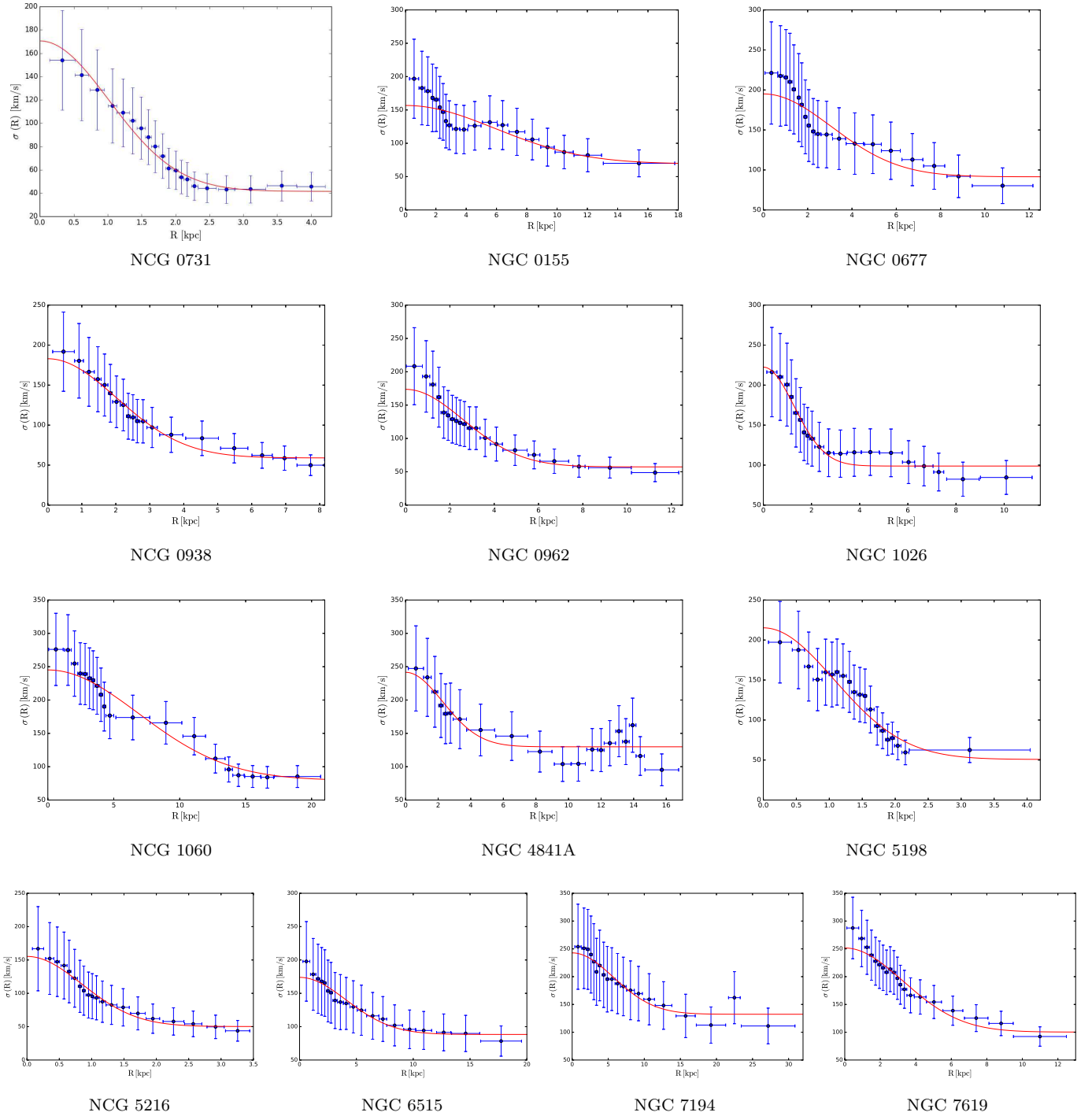


Figure 2. Projected velocity dispersion profiles for the 13 elliptical of our sample, as a function of radial distance in the system, with vertical error bars showing the 1σ dispersion at each radial bin. The solid curve gives the best fit to the universal profile proposed.

gorithm to estimate the parameters, and obtain self-consistent 1σ confidence intervals, which are reported in Table 1. We have trimmed the total sample used in Hernandez et al. (2013a) to 12 globular clusters where the relative errors in the fitted parameters are in all cases smaller than 50%. This excludes 4 globular clusters with poorly determined velocity dispersion profiles, also keeping the globular cluster sample from growing much beyond the numbers of available well measured systems in the category of low rotation elliptical galaxies. This last to ensure that the systematics relevant to any particular class of objects do not dominate and bias the overall comparisons we attempt.

Figure 1 provides the observed velocity dispersion profiles for the Galactic globular clusters of our sample with the best fit to Equation (6) for each system, showing clearly an excellent empirical representation of the measured profiles. A clear decline in the Newtonian inner region is evident, followed by a transition to a ‘‘Tully-Fisher’’ flat asymptote.

3.2. Elliptical galaxies

A sample of low rotation elliptical galaxies was obtained from Sánchez et al. (2016b), in which 200 radial 2D velocity dispersion profiles were produced from the second data release of the CALIFA survey (Sánchez et al. 2012; Walcher et al. 2014; Sánchez et al. 2016a) using the PIPE 3D tool. To ensure that the selected sub-sample was composed of systems with the least dynamical support besides velocity dispersion, we selected galaxies based on their morphology (E0-E3). Our sample comprises only extremely slow rotators, with an average value of a maximum rotation velocity to central sigma per galaxy of $V_{max}/\sigma_0 = 0.213$, very early type systems with negligible total gas content.

We use data directly obtained from Sánchez et al. (2016b), consisting of 2D radial stellar velocity dispersion observations with their respective uncertainties, as well as associated flux for a correct weighted statistical development. From the 2D velocity dispersion observations we extract a projected radial velocity dispersion representation. Due to the large number of pointings in each galaxy, we averaged the projected velocity dispersion observations within 20 radial bins (Figure 2), each with a corresponding 1σ dispersion which greatly overshadows the intrinsic observational error for each data point. In spite of the high 1σ dispersion towards the center of the galaxies, we adopt this method for statistical consistency with the globular clusters treated. Monte Carlo generated errors for each data point are only about 15 km/s, while the radial bin average confidence intervals can reach up to 50 km/s. As described in Sanchez et al. (2016a,b) velocity dispersion measurements of under 40 km/s from the middle resolu-

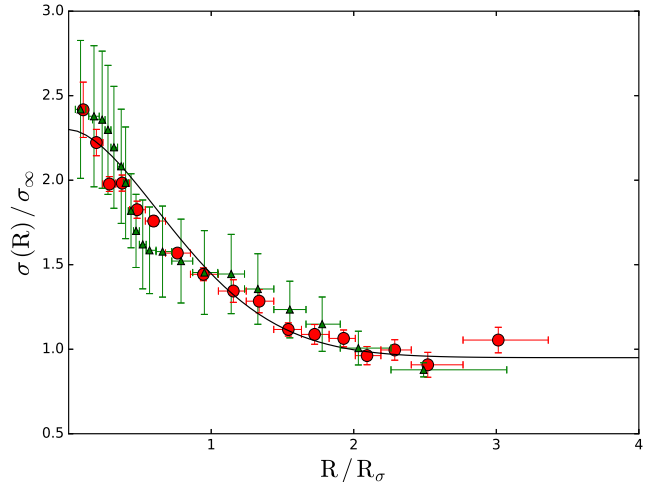


Figure 3. Observed projected velocity dispersion profiles in units of the corresponding σ_∞ values as a function of radius normalized to the corresponding R_σ values, for two distinct systems. Red circles correspond to measurements for the Galactic globular cluster NGC 5139, with a central velocity dispersion of 15.2km/s and $R_\sigma = 16.7\text{pc}$. Green triangles correspond to the elliptical galaxy NGC 0677, with a central velocity dispersion of 195km/s and $R_\sigma = 4.3\text{kpc}$. The consistency of the two scaled projected velocity dispersion profiles is evident, despite the range of scales covered by the comparison.

tion setup V1200 are not reliable, so we have discarded these data points in our estimates. Using again a non-linear least squares Levenberg-Marquardt algorithm, we fit the proposed universal function of Equation (6) to the projected velocity dispersion profiles and obtain optimal parameters as well as their respective confidence intervals. After discarding various systems with poorly determined parameters, with fractional errors larger than 50% in the fitted parameters, we compile a final sample of 13 elliptical galaxies, as reported in Table 1.

Figure 2 shows the radial binning of the projected 2D radial velocity dispersion of the elliptical galaxies in the sample, as well as the best fit to the universal function of Equation (6). Note again the suitability of the fits in all cases.

Although the general fit of the proposed universal velocity dispersion profile is clearly very good across the range of objects treated (see the full figure set), specially towards the flattened outer regions, it is also clear that in a number of both globular clusters and elliptical galaxies, a slight central enhancement in the data with respect to the fitted function appears. This cuspy velocity dispersion profiles, e.g. the globular cluster NGC 2419 and elliptical galaxies NGC 0962 and NGC 1060, could signal the presence of a central black hole. This is a common feature in early type galaxies, and could also appear in globular clusters. For example, Baumgardt (2017) recently concluded from dynamical studies

Table 1. Parameters for velocity dispersion profiles of the the pressure supported systems.

Type of system	Identification	$\sigma_0(km/s)$	$\sigma_\infty(km/s)$	$R_\sigma(pc)$
Globular Cluster	NGC 0104	4.5 ± 0.4	5.0 ± 0.1	14.8 ± 0.9
Globular Cluster	NGC 1851	4.1 ± 1.7	3.9 ± 0.4	7.9 ± 2.3
Globular Cluster	NGC 1904	2.4 ± 0.6	2.0 ± 0.4	10.3 ± 3.3
Globular Cluster	NGC 2419	4.7 ± 0.8	1.0 ± 0.4	1.8 ± 0.3
Globular Cluster	NGC 5139	8.0 ± 0.7	7.2 ± 0.4	16.7 ± 1.9
Globular Cluster	NGC 6171	1.4 ± 0.4	2.7 ± 0.2	3.8 ± 1.1
Globular Cluster	NGC 6218	3.3 ± 0.9	1.4 ± 0.5	4.7 ± 1.2
Globular Cluster	NGC 6341	3.8 ± 0.7	3.1 ± 0.4	6.9 ± 1.4
Globular Cluster	NGC 6656	3.8 ± 1.3	3.3 ± 0.8	7.4 ± 1.7
Globular Cluster	NGC 6752	3.5 ± 0.8	2.0 ± 0.3	10.7 ± 1.4
Globular Cluster	NGC 7078	5.1 ± 1.0	3.0 ± 0.3	8.7 ± 1.7
Globular Cluster	NGC 7099	1.8 ± 0.5	2.2 ± 0.3	6.2 ± 2.3
Elliptical Galaxy	NGC 0155	87.6 ± 25.5	69.1 ± 25.4	$(8.4 \pm 3.6) \times 10^3$
Elliptical Galaxy	NGC 0677	103.6 ± 24.4	91.4 ± 16.7	$(4.3 \pm 1.6) \times 10^3$
Elliptical Galaxy	NGC 0731	129.0 ± 26.9	41.6 ± 6.6	$(1.4 \pm 0.2) \times 10^3$
Elliptical Galaxy	NGC 0938	124.0 ± 25.8	59.0 ± 7.0	$(2.9 \pm 0.5) \times 10^3$
Elliptical Galaxy	NGC 0962	116.3 ± 22.5	57.3 ± 8.5	$(3.7 \pm 0.8) \times 10^3$
Elliptical Galaxy	NGC 1026	123.6 ± 37.7	98.8 ± 8.8	$(1.8 \pm 0.4) \times 10^3$
Elliptical Galaxy	NGC 1060	165.6 ± 18.8	79.5 ± 16.7	$(9.7 \pm 2.0) \times 10^3$
Elliptical Galaxy	NGC 4841A	111.7 ± 46.7	129.9 ± 8.9	$(3.2 \pm 1.4) \times 10^3$
Elliptical Galaxy	NGC 5198	163.6 ± 27.3	53.8 ± 14.7	$(1.5 \pm 0.2) \times 10^3$
Elliptical Galaxy	NGC 5216	105.1 ± 28.3	50.2 ± 9.6	$(1.2 \pm 0.3) \times 10^3$
Elliptical Galaxy	NGC 6515	85.6 ± 24.3	88.4 ± 13.5	$(5.8 \pm 2.2) \times 10^3$
Elliptical Galaxy	NGC 7194	110.4 ± 33.6	132.3 ± 18.7	$(8.0 \pm 3.2) \times 10^3$
Elliptical Galaxy	NGC 7619	151.3 ± 21.8	100.3 ± 14.7	$(4.6 \pm 0.9) \times 10^3$

The first two columns give the object class and identifier for the systems studied. The following three entries show the parameters of the fits to the observed projected velocity dispersion profiles and their confidence intervals. Data from the Scarpa et al. group and the Lane et al. group for Galactic globular clusters, and data from the CALIFA collaboration for elliptical galaxies.

of NGC 5139 that this cluster likely harbors a 40,000 solar mass black hole in its center. From Figure 1 we see that indeed, this particular system shows the most prominent central velocity dispersion excess with respect to the universal profile fitted of all the globular clusters treated.

Fortunately, this inner velocity dispersion excesses are very central features which do not affect the determinations of R_σ or σ_∞ , the parameters which can be associated to MONDian dynamical predictions.

4. COMPARISONS WITH MONDIAN EXPECTATIONS

Comparing Figures 1 and 2, we see that although the physical scale is changing from pc to kpc, the velocity profiles of globular clusters and ellipticals can both be fitted adequately by the same family of functions. Further, while the peak σ_0 is on average different for glob-

ular clusters and ellipticals when scaled with σ_∞ , the transition from a declining velocity profile to a flat one emerges with remarkable consistency at a scaled radius of $R/R_\sigma \sim 2$.

From Equation (6) we see that the central velocity dispersion values, given by $\sigma(0) = \sigma_0 + \sigma_\infty$, span two orders of magnitude, with the scale radii R_σ covering three orders of magnitude, and the total baryonic masses going from a few $10^4 M_\odot$ scale for the smallest Galactic globular clusters to $10^{11} M_\odot$ for the elliptical galaxies. If we now scale the projected velocity dispersion profiles of the various systems presented in the previous section, and consider $\sigma(R)/\sigma_\infty$ as a function of R/R_σ for each profile, only one degree of freedom remains, given by the central velocity dispersion, $\sigma(0)/\sigma_\infty$.

Therefore, if we choose distinct systems having equal $\sigma(0)/\sigma_\infty$ values, they should look identical in a $\sigma(R)/\sigma_\infty$ vs. R/R_σ plot. Figure 3 shows the scaled velocity dis-

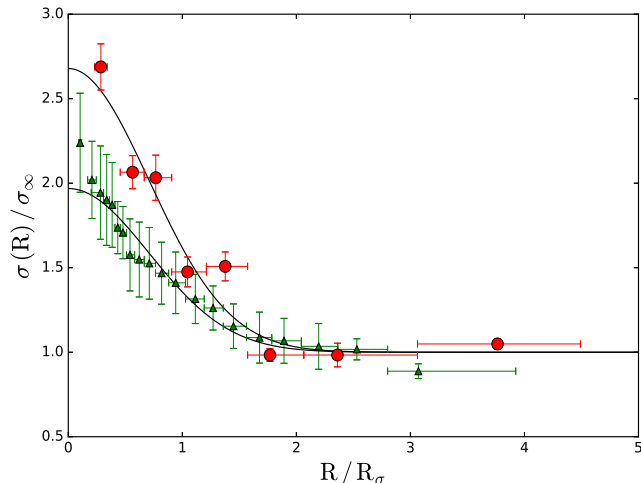


Figure 4. Observed projected velocity dispersion profiles in units of the corresponding σ_∞ values as a function of radius normalized to the corresponding R_σ values, for two distinct systems. Red circles correspond to measurements for the Galactic globular cluster NGC 7078, with a central velocity dispersion of 8.1km/s and $R_\sigma = 8.7\text{pc}$. Green triangles show the elliptical galaxy NGC 6515, with a central velocity dispersion of 174km/s and $R_\sigma = 5.8\text{kpc}$. The two scaled profiles can be modeled through the same functional form of the proposed universal profile, the Figure also shows the tendency for the scaled profiles of elliptical galaxies to be flatter and for globular clusters to be steeper.

persion profiles of two different systems chosen to have very similar $\sigma(0)/\sigma_\infty$ values. Circles correspond to the Galactic globular cluster NGC 5139, while triangles represent data for the elliptical galaxy NGC 0677. The solid line shows a fit to Equation (6) for the combined data set, the self-similarity of the two quite distinct pressure supported systems is evident; once scaled, both observed velocity dispersion data samples are consistent with each other to within their respective confidence intervals. Actual physical radial scales vary from $R_\sigma = 16.7\text{pc}$ of the globular cluster shown to $R_\sigma = 4.3\text{kpc}$ of the elliptical galaxy. We see pressure supported systems as showing a simple empirical kinematic profile across many orders of magnitude in scale and distinct classes of systems.

Despite the overlap evident in Figure 3, typically we find velocity dispersion profiles for elliptical galaxies to be rather flat, while those of Galactic globular clusters tend to be steeper. This is illustrated in Figure 4, which is analogous to Figure 3, but shows more typical examples for the two astrophysical systems analyzed, the Galactic globular cluster NGC 7078 and the elliptical galaxy NGC 6515. Although the same functional form is evident, the degree of central concentration clearly varies as mentioned above.

Regarding Galactic globular clusters, it has been suggested that the flattening of the velocity dispersion profiles could be due to standard Newtonian physics, in

particular tidal heating from the overall Milky Way potential (Küpper 2010). Fortunately, 10 of the globular clusters included in our study form part of a wider sample for which not only distances but also well measured proper motions are available. Indeed, Allen et al. (2006) and Allen et al. (2008) calculated orbital properties for a large sample of 54 Galactic globular clusters within a fully consistent Newtonian galactic model including baryonic disk, bulge and stellar halo, as well as a dominant dark matter halo. In those studies, the authors calculate detailed tidal radii for all globular clusters, not under any 'effective mass' approximation, but through fully calculating the derivative of the total Galactic gravitational force, including evaluating the gradients in acceleration across the extent of the clusters, along the entire orbital trajectories.

In Hernandez et al. (2013a) one of us used fits to Equation (6) to obtain R_σ for Galactic globular clusters including the ones in our present study, with the exception of NGC 2419, to compare with the Newtonian tidal radii of Allen et al. (2006) and Allen et al. (2008). For the globular clusters in our present study (excluding NGC 2419) the ratio of the Newtonian tidal radii - at peri-Galacticon - to R_σ ranges from between 3 to 14.7, with a mean value of 7.1. Thus, it appears extremely unlikely that Newtonian tides are responsible for the flattening observed. The case of NGC 2419 is also clear, proper motions have only recently become available due to the extreme distance at which it finds itself, Massari et al. (2016) provided the first proper motion studies for this cluster, and orbital integration within a Newtonian Galactic potential to show its galactocentric radius oscillates between 53 and 98 kpc, making it highly insensitive to Galactic tides. In going to MONDian schemes, as the gravitational force falls with R^{-1} rather than R^{-2} , the gradient of it is much reduced, and Galactic globular clusters become more robust to Galactic tides than under Newtonian dynamics (e.g. Hernandez & Jimenez 2012), justifying their treatment here as isolated systems.

For the case of the elliptical galaxies in the sample, we use two different criteria to determine interaction and isolation. The first comes directly from the morphological classification of the CALIFA 3rd data release, which is essentially a visual examination of the optical images of each object made by five different CALIFA members, where signs of mergers or interactions were sought. All our sample galaxies except one, NGC 4841A, appear as isolated under this criterion. In a second test, the f parameter discussed in Varela et al. (2004) is calculated for all CALIFA galaxies (Walcher et al. 2014), which is an estimate of the logarithmic ratio between inner and tidal forces acting upon each galaxy, given in terms of the projected distance between target and

neighbor galaxies, the size of the target galaxy and the ratio of their masses as estimated from total luminosities assuming a constant mass-to-light ratio. Galaxies with f values lower than -4.5 are considered completely isolated, while galaxies with $f < -2$ are considered as not affected by tidal forces of their neighboring galaxies. Again, all the galaxies from our sample except for NGC 4841A show f values lower than -2 , indicating no tidal effects are evident upon them. In the case of NGC 4841A, which shows clear visual signs of interaction and has a value of $f = -0.01$, a distinct perturbation in its velocity dispersion profile observations can be observed at around 12-14 kpc. The fit shown includes this slightly perturbed region, indicating the robustness of the fit to details; excluding all data beyond 12 kpc yields fit parameters well within the reported confidence intervals of those resulting from using the full data sample.

Other Newtonian explanations for the flattening in the globular cluster velocity dispersion profiles have been put forward in the literature, e.g. Kennedy (2014) showed that internal N-body relaxation processes can yield results consistent with observations. However, under any Newtonian explanation, it would then be down to a curious coincidence that the amplitude of σ_∞ should scale with the total mass of the clusters in question (as inferred from detailed population synthesis models tuned to the particular ages and metallicities of each from McLaughlin & van der Marel 2005) in consistency with MONDian "Tully-Fisher" expectations, Equation (3), as shown in Hernandez et al. (2013a).

We end this section with Figure 5, which contains the principal result of our study. The Figure shows R_σ and σ_∞ values for the fits to both of the pressure supported systems treated, in a logarithmic plane. The systems shown cover a range of $1.4 - 165.6 km/s$ in central velocity dispersion and $1.8 pc - 9.7 kpc$ in the scale radius R_σ . The two distinct classes of objects are evident, with the small Galactic globular clusters appearing at the low σ_∞ extreme as circles and triangles giving results for elliptical galaxies. The solid line is not a fit to the data but gives the $R_M = 3\sigma_\infty/a_0$ prediction of MONDian gravity of Equation (4).

In going from volumetric velocity dispersion profiles to the observable projected velocity dispersion profiles, various projection effects intervene, in ways which depend on the details of the degree of central concentration of the volumetric velocity dispersion profile, and the real space density profiles of the tracers being analyzed (Hernandez & Jimenez 2012; Jimenez et al. 2013a; Tortora 2014). Such details of the integration implicit in obtaining the line of sight projected profiles we treat necessarily introduce changing systematics across both classes of systems, from the centrally peaked kinematics of globular clusters to the flatter ones of elliptical galax-

ies. To the above we must add the systematics inherent to any comparison across such distinct astrophysical systems over such a range of distances and observational techniques as what we are attempting here. We thus find it encouraging of the physical interpretation presented that the overall trend evident in Figure 5 can be clearly well represented by the predictions of Equation (4), under the natural identification of $R_\sigma = R_M$, the transition to the flat velocity dispersion regime being given by the length scale of MONDian gravity.

We also performed a weighted linear fit to the data in Figure 5 to equation:

$$\left(\frac{R_\sigma}{pc}\right) = A \left(\frac{\sigma_\infty}{km/s}\right)^n. \quad (7)$$

Such a linear fit to the full data set of Figure 5, shown by the dashed line, yields $A = 0.73 \pm 0.13$ and $n = 1.89 \pm 0.32$, in clear accordance with the MONDian predictions of Equation (5) for $A = 0.81$ and $n = 2$. The corresponding fit to only the elliptical galaxies is largely unconstrained, but if we consider only the globular clusters we obtain $A_{GC} = 1.54 \pm 2.35$ and $n_{GC} = 1.45 \pm 1.12$. This is not in conflict with the predictions of Equation 5, although the overall trend is clearly driven by the positions of the two clouds of points coming from the two distinct scale limited classes considered.

Under Newtonian gravity, the flattening observed in elliptical velocity dispersion profiles, where tides are not relevant, would be interpreted as evidence for a dark matter halo, and the consistency of $R_\sigma \propto \sigma^2$ of Figure (5), as another curious coincidence down to the details of biasing and stellar feedback.

Within MOND as such, for systems under the influence of an external gravitational field, a regime change is expected according to whether the internal acceleration of the system in question is smaller or larger than the external one. In fact, if the external acceleration dominates and is larger than a_0 , the system being treated will behave in an essentially Newtonian manner, even if internal accelerations are well below a_0 (Famaey & McGaugh 2012). While not relevant for elliptical galaxies, the collection of Galactic globular clusters treated here span the above MOND transition, some of the closer ones would be expected to be affected by this so called external field effect, while the more distant, e.g. NGC 2419, would be exempt from it, Sanders (2012). From Figure 5 it is clear that all clusters are consistent with the first order MONDian expectations of Equation (4), regardless of their galactocentric distances. Our results hence appear to support generic MONDian schemes where the external field effect might not appear, or result in milder distortions than what appear in MOND as such, e.g. Verinde (2016) or Barrientos & Mendoza

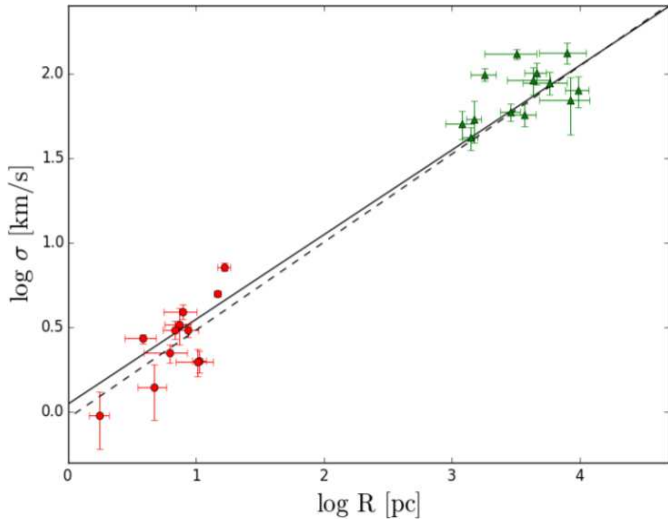


Figure 5. σ_∞ vs. R_σ values for both of the systems treated, red circles for Galactic globular clusters and green triangles for low rotation elliptical galaxies, in a logarithmic plane. The solid line is not a fit to the data, it rather shows the MONDian expectations of Equation (4) for the predicted scaling of $R_M = 3\sigma_\infty^2/a_0$, $R_M/pc = 0.81(\sigma_\infty/kms^{-1})^2$. A linear regression fit (dashed line) gives $R_\sigma = (0.73 \pm 0.13)\sigma_\infty^{1.89 \pm 0.32}$, clearly compatible with the theoretical expectation under the identification of $R_\sigma = R_M$.

(2016).

It appears that a unique gravitational physics applies, with a clear transition radius at a R_M scale where the decline of the inner Newtonian $R < R_M$ region gives way to the ‘‘Tully-Fisher’’ $\sigma(R) \propto (GMa_0)^{1/4}$ of the outer MONDian region, regardless of the fact that we start with self-gravitating systems of stars at pc scales, to the much larger ellipticals at kpc scales.

Increasing our sample size and extending the sample with other type of pressure supported systems, e.g. dSphs, to validate our conclusions is evidently a desirable development, which however must be undertaken with care to keep the number of objects at each class considered relatively balanced, to make sure that the

systematics inherent to any particular class are not biasing conclusions. Similarly, filling the gap present at σ_∞ values of between 10 and 40 km/s would be highly desirable.

5. CONCLUSIONS

A universal projected velocity dispersion profile of $\sigma(R) = \sigma_0 e^{-(R/R_\sigma)^2} + \sigma_\infty$ has been shown to accurately model two distinct classes of astronomical systems; globular clusters and low rotation elliptical galaxies.

MONDian gravity generically predicts $R_M = 3\sigma_\infty^2/a_0$, $R_M/pc = 0.81(\sigma_\infty/kms^{-1})^2$. Data across 7 orders of magnitude in mass give $R_\sigma/pc = A(\sigma_\infty/kms^{-1})^n$, with $A = 0.73 \pm 0.13$ and $n = 1.89 \pm 0.32$.

Thus, in spite of significant observational uncertainties and varying projection effects across apparently very different classes of astronomical systems, the identification of the local physical R_M radius with the empirical projected kinematic R_σ parameter yields results consistent with generic modified gravity expectations, where gravitational anomalies in the $a < a_0$ regime stem from changes in the physics and not a hypothetical dark matter component.

ACKNOWLEDGEMENTS

The authors acknowledge constructive criticism from an anonymous referee as important towards reaching a clearer and more complete revised version of this manuscript. Xavier Hernandez acknowledges financial assistance from UNAM DGAPA grant IN100814. Reginaldo Durazo acknowledges financial assistance from a CONACyT scholarship. Bernardo Cervantes Sodi acknowledge financial support through PAPIIT project IA103517 from DGAPA-UNAM. SFS thanks the CONACyT-125180, DGAPA-IA100815 and DGAPA-IA101217 projects for providing him support in this study.

REFERENCES

- Abell, G. O. 1958, ApJS, 3, 211
 Allen, C., Moreno, E., & Pichardo, B. 2006, ApJ, 652, 1150
 Allen, C., Moreno, E., & Pichardo, B. 2008, ApJ, 674, 237-246
 Barkhouse, W. A., Yee, H. K. C., & López-Cruz, O. 2007, ApJ, 671, 1471
 Barrientos, E., & Mendoza, S. 2016, arXiv:1612.07970
 Baumgardt, H. 2017, MNRAS, 464, 2174
 Bekenstein, J. D. 2004, Phys. Rev. D, 70, 083509
 Binney, J., & Tremaine, S. 1987, Princeton, NJ, Princeton University Press, 1987, 747 p.,
 Bower, R. G., Lucey, J. R., & Ellis, R. S. 1992, MNRAS, 254, 601
 Capozziello, S., & de Laurentis, M. 2011, Phys. Rep., 509, 167
 Cappellari, M., Bacon, R., Bureau, M., et al. 2006, MNRAS, 366, 1126
 Chae, K.-H., & Gong, I.-T. 2015, MNRAS, 451, 1719
 Dabringhausen, J., Kroupa, P., Famaey, B., & Fellhauer, M. 2016, MNRAS, 463, 1865
 Desmond, H. 2017, MNRAS, 464, 4160
 Emsellem, E., Cappellari, M., Krajnović, D., et al. 2011, MNRAS, 414, 888
 Emsellem, E., Cappellari, M., Peletier, R. F., et al. 2004, MNRAS, 352, 721
 Famaey, B., & McGaugh, S. S. 2012, Living Reviews in Relativity, 15, 10
 Famaey, B., & Binney, J. 2005, MNRAS, 363, 603
 Gentile, G., Famaey, B., Angus, G., & Kroupa, P. 2010, A&A, 509, A97
 Hernandez, X., & Jiménez, M. A. 2012, ApJ, 750, 9
 Hernandez, X., Jiménez, M. A., & Allen, C. 2013a, ApJ, 770, 83
 Hernandez, X., Jiménez, M. A., & Allen, C. 2013b, MNRAS, 428, 3196

- Jiménez, M. A., García, G., Hernandez, X., & Nasser, L. 2013, *ApJ*, 768, 142
- Jones, C., & Forman, W. 1999, *ApJ*, 511, 65
- Kennedy, G. F. 2014, *MNRAS*, 445, 4446
- Küpper, A. H. W., Kroupa, P., Baumgardt, H., & Heggie, D. C. 2010, *MNRAS*, 401, 105
- Lane, R. R., Kiss, L. L., Lewis, G. F., et al. 2011, *A&A*, 530, A31
- Lane, R. R., Kiss, L. L., Lewis, G. F., et al. 2010, *MNRAS*, 401, 2521
- Lane, R. R., Kiss, L. L., Lewis, G. F., et al. 2009, *MNRAS*, 400, 917
- Lane, R. R., Kiss, L. L., Lewis, G. F., et al. 2010, *MNRAS*, 406, 2732
- Lelli, F., McGaugh, S. S., Schombert, J. M., & Pawlowski, M. S. 2016, accepted for publication in *ApJ*, arXiv:1610.08981
- Massari, D., Posti, L., Helmi, A., Fiorentino, G., & Tolstoy, E. 2016, accepted for publication in *A&A Letters*, arXiv:1612.00183
- McGaugh, S. S. 2012, *AJ*, 143, 40
- McGaugh, S. S., Lelli, F., & Schombert, J. M. 2016, *Physical Review Letters*, 117, 201101
- McLaughlin, D. E., & van der Marel, R. P. 2005, *ApJS*, 161, 304
- Mendoza, S., Bernal, T., Hernandez, X., Hidalgo, J. C., & Torres, L. A. 2013, *MNRAS*, 433, 1802
- Mendoza, S., Hernandez, X., Hidalgo, J. C., & Bernal, T. 2011, *MNRAS*, 411, 226
- Milgrom, M. 1983, *ApJ*, 270, 365
- Milgrom, M. 1984, *ApJ*, 287, 571
- Richtler, T., Schuberth, Y., Hilker, M., et al. 2008, *A&A*, 478, L23
- Rodrigues, D. C., de Oliveira, P. L., Fabris, J. C., & Gentile, G. 2014, *MNRAS*, 445, 3823
- Samurović, S. 2014, *A&A*, 570, A132
- Samurović, S. 2016, *Ap&SS*, 361, 199
- Sánchez, S. F., García-Benito, R., Zibetti, S., et al. 2016a, *A&A*, 594, A36
- Sánchez, S. F., Pérez, E., Sánchez-Blázquez, P., et al. 2016b, *Rev. Mexicana Astron. Astrofis.*, 52, 171
- Sánchez, S. F., Kennicutt, R. C., Gil de Paz, A., et al. 2012, *A&A*, 538, A8
- Sanders, R. H. 2012, *MNRAS*, 419, L6
- Sanders, R. H., & McGaugh, S. S. 2002, *ARA&A*, 40, 263
- Scarpa, R., & Falomo, R. 2010, *A&A*, 523, A43
- Scarpa, R., Marconi, G., Carraro, G., Falomo, R., & Villanova, S. 2011, *A&A*, 525, A148
- Scarpa, R., Marconi, G., Gilmozzi, R., & Carraro, G. 2007, *A&A*, 462, L9
- Scarpa, R., Marconi, G., Gilmozzi, R., & Carraro, G. 2007, *The Messenger*, 128,
- Serra, A. L., Diaferio, A., Murante, G., & Borgani, S. 2011, *MNRAS*, 412, 800
- Swaters, R. A., Sanders, R. H., & McGaugh, S. S. 2010, *ApJ*, 718, 380
- Tian, Y., & Ko, C.-M. 2016, *MNRAS*, 462, 1092
- Tortora, C., Romanowsky, A. J., Cardone, V. F., Napolitano, N. R., & Jetzer, P. 2014, *MNRAS*, 438, L46
- Varela, J., Moles, M., Márquez, I., et al. 2004, *A&A*, 420, 873
- Verlinde, E. P. 2016, arXiv:1611.02269
- Walcher, C. J., Wisotzki, L., Bekeraité, S., et al. 2014, *A&A*, 569, A1
- Wolf, J., Martinez, G. D., Bullock, J. S., et al. 2010, *MNRAS*, 406, 1220
- Yahil, A., & Vidal, N. V. 1977, *ApJ*, 214, 347
- York, D. G., Adelman, J., Anderson, J. E., Jr., et al. 2000, *AJ*, 120, 1579

